Interannual variability in intercontinental transport

Mohan Gupta[(1)], Anne Douglass[(2)], S. Randy Kawa[(2)] and Steven Pawson[(3)]

[(1)]GEST/NASA GSFC, Code 916, Greenbelt, MD 20771

[(2)]NASA GSFC, Code 916, Greenbelt, MD 20771

[(3)]GEST/NASA GSFC, GMAO, Greenbelt, MD 20771

To be submitted to Geophysical Research Letters

Summary

We have investigated the importance of intercontinental transport using source-receptor relationship. A global radon-like and seven regional tracers were used in three-dimensional model simulations to quantify their contributions to column burdens and vertical profiles at world-wide receptors. Sensitivity of these contributions to meteorological input was examined using different years of meteorology in two atmospheric simulations. Results show that Asian emission influences tracer distributions in its eastern downwind regions extending as far as Europe with major contributions in mid- and upper troposphere. On the western and eastern sides of the US, Asian contribution to annual average column burdens are 37% and 5% respectively with strong monthly variations. At an altitude of 10 km, these contributions are 75% and 25% respectively. North American emissions contribute more than 15% to annual average column burden and about 50% at 8 km altitude over the European region. Contributions from tropical African emissions are wide-spread in both the hemispheres. Differences in meteorological input cause non-uniform redistribution of tracer mass throughout the troposphere at all receptors. We also show that in model-model and model-data comparison, correlation analysis of tracer's spatial gradients provides an added measure of model's performance.

Interannual variability in intercontinental transport

Mohan Gupta[(1)], Anne Douglass[(2)], S. Randy Kawa[(2)] and Steven Pawson[(3)]

[(1)]GEST/NASA GSFC, Code 916, Greenbelt, MD 20771

[(2)]NASA GSFC, Code 916, Greenbelt, MD 20771

[(3)]GEST/NASA GSFC, GMAO, Greenbelt, MD 20771

To be submitted to Geophysical Research Letters

August 19, 2003

ABSTRACT

We have investigated the importance of intercontinental transport using source-receptor relationship. A global radon-like and seven regional tracers were used in three-dimensional model simulations to quantify their contributions to column burdens and vertical profiles at world-wide receptors. Sensitivity of these contributions to meteorological input was examined using different years of meteorology in two atmospheric simulations. Results show that Asian emission influences tracer distributions in its eastern downwind regions extending as far as Europe with major contributions in mid- and upper troposphere. On the western and eastern sides of the US, Asian contribution to annual average column burdens are 37% and 5% respectively with strong monthly variations. At an altitude of 10 km, these contributions are 75% and 25% respectively. North American emissions contribute more than 15% to annual average column burden and about 50% at 8 km altitude over the European region. Contributions from tropical African emissions are wide-spread in both the hemispheres. Differences in meteorological input cause non-uniform redistribution of tracer mass throughout the troposphere at all receptors. We

also show that in model-model and model-data comparison, correlation analysis of tracer's spatial gradients provides an added measure of model's performance.

INTRODUCTION

Intercontinental transport (ICT) dominates dispersion and regional loading of short-lived air pollutants e.g. aerosols and ozone. Besides being fundamental to urban air pollution, these short-lived species play vital role in global as well as regional climate forcings [*Hansen et al.*, 2000; Giorgi *et al.*, 2002]. Therefore, ICT can be considered as one of the mechanisms that interlink air quality with climate change. Recent observational analyses and modeling results have conclusively shown the impact of increasing Asian emissions of air pollutants on the background ozone over the western US [*Fiore et al.*, 2002; *Jaffe et al.*, 2003]. This role of ICT in the regional context will become increasingly important due to ongoing latitudinal shift in emissions of air pollutants from developed countries to tropical developing countries [*Gupta et al.*, 1998; *Prather et al.*, 2003] where both convective and photochemical activities are very intensive. In fact, *Holloway et al.* [2003] have even proposed an idea of a hemispheric treaty to simultaneously address issues of both air quality and climate change. Moreover, two ongoing atmospheric campaigns INTEX [*Singh et al.*, 2003] and IGAC-ITCT [http://www.al.noaa.gov/WWWHD/pubdocs/ITCT] have been specially designed to understand ICT and its influence on northern hemispheric air pollution.

Interannual variations in dynamics and circulation are inherent to the atmosphere and are expected to influence ICT as well as regional chemical composition. Without being specific to a particular choice, atmospheric chemical transport models (CTMs) have often recycled a single year's meteorology over multiple years to produce constituent fields. Simulated constituent

fields have been compared with observations and with fields produced by other CTMs that may use different meteorological data. Conclusions drawn on model's performance from these comparison studies may be premature unless the sensitivity of model results with regard to meteorological input is examined. Recently, some attention has been given to this important aspect of atmospheric modeling. For example, annually varying meteorological inputs have been used to deduce time-dependent emissions of CH_4 [*Dentener et al.*, 2002] and CO_2 [*Rodenbeck et al.*, 2003] and also to interpret observed interannual variations in atmospheric CO [*Allen et al.*, 1996], CH_4 [*Warwick et al.*, 2002, *Dentener et al.*, 2003] and interhemispheric gradient in CO_2 [*Dargaville et al.*, 2003].

Despite the stated importance of ICT and meteorological input in dispersion of air pollutants, there remain uncertainties in identifying and quantifying temporally varying contributions of regional emissions to their atmospheric burdens at receptor locations. In addition, it is not clear to what extent magnitudes of these contributions are affected by the meteorological variability. These uncertainties make it difficult to reconcile the differences noted in model-model and model-data comparison studies, and also in deduction of surface emissions using 'inversion techniques'.

There are two-fold objectives of this study. Firstly, what are the contributions of regional sources of a tracer to its atmospheric distribution at receptor locations and how these contributions vary in space and time. Secondly, how much sensitive is ICT, and hence these contributions, with respect to meteorological input. We have used an approach of 'tagging' of regional emissions. Besides analyzing the source-receptor relationship, this approach helps in examining sensitivities due to model inputs, e.g. meteorology, and in constraining uncertainty in emissions based on their specificity. Additionally, analysis of tagged atmospheric loadings of air

pollutants provides valuable input in devising observational strategies, developing and implementing emission control strategies and formulating technology transfer initiatives.

MODEL SIMULATIONS

Two simulations of global and regional radon-like tracers were performed using the Goddard Space Flight Center (GSFC) off-line three-dimensional parameterized chemistry and transport model (PCTM) [*Nielsen and Douglass*, 2001]. Both of these simulations differ from each other due to different sets of meteorological input to the model. For two consecutive years, meteorological fields (surface pressure, temperature and winds), and convective and diffusive fluxes input were adopted from the NASA-NCAR Finite Volume General Circulation Model (FVGCM). Operational details for FVGCM and PCTM are given elsewhere [*Douglass et al.*, 2003; *Gupta et al.*, 2003].

A global tracer (O) as well as seven other tracers with regionally tagged emissions representative of Indo-China (A), North America (B), Europe (C), Africa (D), South America (E), Russia (F) and Australia (G), as shown in Figure 1, were used in model simulations. Land-based and oceanic surface emissions for tracer O were prescribed based on *Jacob et al.* [1997]. Figure 1 displays percent of the global emissions covered by each regional tracer. Altogether seven regional tracers account for about 90% of the global emissions for tracer O. All tracers were treated chemically non-interactive (so that their masses can be linearly added) with 'invariable' atmospheric lifetime of 5.6 days. This lifetime is comparable to tropospheric zonal mixing time and to lifetimes of aerosols and ozone precursors (e.g. NOx).

We identified 45 regions around the globe as receptors of all 8 tracers. However, we will concentrate on two receptors, R42 and R43, which were placed at (135°W, 14-50°N) and (60°W,

14-50°N) respectively (see Figure 1). Longitudinally, R42 and R43 can be considered as entry and exit receptors of non-North American emissions to region B. Model simulations corresponding to two different year's of meteorological input are termed as Y66 and Y67. Except for the FVGCM input, both model simulations were carried out under all other identical conditions. Simulated tracer distributions for Y66 were considered to be representative of the reference state.

RESULTS AND DISCUSSION

To analyze contributions of regional emissions to tracer distributions over receptors and their meteorological dependence, we focus on two aspects of tracer distributions: (a) column amounts, and (b) vertical profiles. We also use coefficients of correlation to analyze the effect of meteorology on tracer distributions.

a. Column Amounts

For simulation Y66, Table 1 shows relative contributions from regional sources to annual average tracer column burdens for receptors R42 and R43. Emissions from regions A and B contribute more than 60% of the total tracer column burden over R42 with dominant (~37%) contribution from region A. For R43, contribution from region A reduces to about 5% whereas contribution from region B increases to 57%. Emissions from regions F and D contribute more than 10% to the total column burdens over R42 and R43 respectively. Influence of emission from region A can be seen over the Europe where it contributes ~3% to the annual average column burden. The corresponding contribution from region B is about 18%. Due to its tropical location, region D contributes to tracer column amounts in both the hemispheres.

In steady state, calculated global burden for tracer O is the same (0.24 kg of radon) in both simulations Y66 and Y67 but there is significant variability in its regional amounts caused

by differences in meteorological input to the model. Over all 45 receptors, this variability in annual average burden ranges between -8.5% to +13.5% with large magnitudes for receptor regions at remote locations. For receptors R42 and R43, total column burdens of tracer O from simulation Y67 differ by +1.4% and -3.2% respectively when compared with those from simulation Y66. These differences (DIF) are computed using $(C_{Y66}-C_{Y67})*100/C_{Y67}$, where at a given receptor C_{Y66} and C_{Y67} are column amounts of a tracer from simulations Y66 and Y67 respectively. We found strong monthly variability in DIF for monthly averaged column burdens for receptors R42 and R43 as shown in Figure 2. Over a year, DIF for R42 and R43 range between (-15% to +34%) and (-15% to +13%) respectively. It is important to note that there are several months (e.g. July-September) in a year when DIF values are exactly opposite in sign for receptors R42 and R43.

Radon-like tracer used in this study is chemically non-interactive, thus strength of its atmospheric distribution can be considered directly proportional to global emissions. In other words, if one were to nullify the magnitude of DIF at a given receptor solely in terms of surface emissions then there are several options that can be considered: (1) change global emissions of a tracer equal to the magnitude of DIF, and (2) change regional emissions to account for differences in amounts of column burdens. For example, discrepancy in annual average column amount for R42 from simulation Y66 and Y67 can be reduced to zero by increasing global emissions in Y67 simulation by 1.4%. Equivalently this can be achieved by increasing regional emissions by either 3.9%, 4.8%, 33.9%, 33.9%, 57.8%, 13.6% for source regions A, B, C, D, E, F, G respectively, or some combination of regional sources. Obviously, besides deviating from the global tracer burden, any adjustment in global or regional emissions will cause 'unwanted'

effects at other receptor locations. For example, stated reduction in tracer emissions will further decrease value of DIF for receptor R43.

We noted strong monthly variation in regional contributions to column burden at all receptors. For example, over a year contributions from region A for Y66 range between (18.5-55.4)% and (2.5-8.8%) for receptors R42 and R43 respectively (see Table 1 for more details). For region B, this contribution ranges between (5.2-41.3)% and (49.4-68.7)% for receptors R42 and R43 respectively. For November, contribution from region A to receptor R42 in Y66 and Y67 are 43% and 20% respectively, whereas, contribution from region B at this receptor in Y66 and Y67 are 35% and 56% respectively indicating further that variability in meteorological input to the model can alone not only redistributes the column burdens but also introduces significant variations in regional contributions.

b. Vertical Profiles

Tagging of regional emissions can also help to interpret vertical profiles in the context of model-model and model-data intercomparison. Based on contribution of regional sources to tracer concentration at various altitudes, tagging approach helps to interpret quality of meteorological input and to constrain the uncertainty in regional emission distributions. Figure 3 shows percent contributions of regional sources to annually averaged vertical profile of tracer O over receptor locations R42 and R43.

Over the receptor R42, contribution from region B for Y66 dominates tracer's vertical profile up to an altitude of ~2km. Above this altitude, relative contribution from region A supercedes that from region B up to an altitude range of ~12km due to convective venting of boundary layer airmass from this region followed by horizontal advection. Between 4-12 km altitude, region A contributes more than 50% to the total concentration of tracer which reaches as

high as 75% at ~10 km altitude. Between surface and 5 km, region F emission contributes more than 10% to the tracer concentration. In the lower and mid troposphere, other minor contributors to vertical profile are regions C and F. As compared to that for Y66, annually averaged vertical profile of tracer O from Y67 differs in the range of -4% to 12% as shown in Figure 4 indicating that meteorological variabilities can introduce non-uniform alterations in vertical profile at a given receptor.

For receptor R43, emissions from region B dominates tracer vertical profile up to an altitude of ~12 km (see Figure 3). Above this altitude, contributions from region E supercedes those from region B. In the lower troposphere, second major contributor to vertical profile is region D which accounts for 10-15% of tracer concentration throughout the troposphere. Above 4 km altitude, contribution from region A is more than 5% which reaches to at much as 25% at an altitude of ~11 km. Annually averaged vertical profile of tracer over R43 from Y67 differs in the range of -9% to 5% when compared against that from Y66 (see Figure 4).

For the annually averaged vertical profile over Europe, local emissions from region C contribute the most between surface and ~4 km. Between 4 and 10 km, region B is the major contributor and it contributes between 35-55% with the maximum at 8 km. Above 10 km, region A contributes the most to annually average vertical profile over Europe.

There are significant monthly variations in regional contribution to vertical profiles of tracer O. For example, contribution from region A to tracer concentration between 10 and 11 km for receptor R42 varies between 40% during January to more than 80% during May. At surface, this contribution from region A varies between 5-20% over a year.

These results collectively indicate that analysis of atmospheric composition at regional receptors must be made in the global context while keeping the importance of ICT in

perspective. At any given time, earth's atmosphere has a unique chemical composition, therefore, global impacts of any adjustment in regional input values in model simulations must be considered. Additionally, composite portrait of tracer distribution (e.g. vertical profile, surface mixing ratios and column amounts) must be considered simultaneously while making comparisons between model-model and model-data. This is particularly important when deducing surface emissions of air pollutants using 'inversion techniques' [*Pak and Prather*, 2001].

c. Tracer Correlations

Coefficients of correlation between tracer concentrations from two different sources (e.g. model vs. model and/or model vs. data) are often used as an indicator of model performance. Extreme ends of absolute value of correlation coefficients i.e. 1 and 0 show the maximum levels of agreement and disagreement respectively. We used coefficient of correlation to intercompare July monthly averaged tracer distributions from simulation Y66 and Y67. Figure 5 shows longitudinal variations in correlation coefficients for absolute mixing ratios and their spatial gradients in all three directions. Correlation coefficients for absolute mixing ratios at all longitudes are more than 0.9 indicating a strong resemblance between tracer distributions from Y66 and Y67. However, spatial gradients show relatively poor correlation with the maximum fluctuation in coefficient values for longitudinal gradients (0.2-0.6) and the minimum for vertical gradient (0.65-0.9). This analysis of correlation coefficients shows that besides considering absolute mixing ratios, associated spatial variations must also be taken into account while making model-model and model-data comparisons.

Our model analyses are specific to tracer's lifetime, chemical reactivity and emission distributions as well as meteorological fields used in the simulations. Any deviations in these input values will have significant effects on the magnitude of results presented here.

CONCLUSIONS

In this study, we have examined the importance of intercontinental transport in dispersing the regionally emitted tracer mass and its dependence on meteorological variability. Results show that contributions from regional emissions to tracer distribution vary strongly with space and time which should be considered while interpreting model-data comparisons. In addition this study demonstrates that differences in meteorological input cause non-uniform alterations in tracer mass throughout the troposphere at all receptors. Both of these factors are important in evaluating the models, and deducing and constraining the emission estimates. Model analysis indicates that in model-model and model-data comparison, correlation of tracer spatial gradients provides an added measure of model's performance.

ACKNOWLEDGEMENTS

This work was supported by NASA's Atmospheric Chemistry Modeling and Analysis Program and the EOS IDS Program.

REFERENCES

Allen, D., P. Kasibhatla, A.M. Thompson, R.B. Rood, B.G. Doddridge, K.E. Pickering, R.D. Hudson and S.-J. Lin, Transport-induced interannual variability of carbon monoxide determined using a chemistry and transport model, *J. Geophys. Res., 101*, 28655-28669, 1996.

Dargaville, R.J., S.C. Doney and I.Y. Fung, Inter-annual variability in the interhemispheric atmospheric CO_2 gradient: contributions from transport and seasonal rectifier, *Tellus, 55B*, 711-722, 2003.

Dentener, F., M. van Weele, M. Krol, S. Houweling and P. van Velthoven, Trends and inter-annual variability of methane emissions derived from 1979-1993 global CTM simulations, *Atmos. Chem. Phys. Discuss., 2*, 249-287, 2002.

Dentener, F., W. Peters, M. Krol, M. van Weele, P. Bergamaschi, and J. Lelieveld, Inter-annual variability and trend of CH4 lifetime as a measure for OH changes in the 1979-1993 time period, J. Geophys. Res., 108(D15), 4442, doi: 10.1029/2002JD002916, 2003.

Douglass, A.R., M.R. Schoeberl and R.B. Rood, Evaluation of transport in the lower tropical stratosphere in a global chemistry and transport model, *J. Geophys. Res., 108*(D9), 4259, doi: 10.1029/2002JD002696, 2003.

Fiore, A. M., D. J. Jacob, I. Bey, R. M. Yantosca, B. D. Field, and J. G. Wilkinson, Background ozone over the United States in summer: origin and contribution to pollution episodes, *J. Geophys. Res., 107*(D15), 10.1029/2001JD000982, 2002.

Giorgi, F., X. Bi and Y. Qian, Direct radiative forcing and regional climatic effects of anthropogenic aerosols over East Asia: A regional coupled climate-chemistry/aerosol model study, *J. Geophys. Res., 107*(D20), 4439, doi:10.1029/2001JD001066, 2002.

Gupta, M.L., R.J. Cicerone and Scott Elliott, Perturbation to global tropospheric oxidizing capacity due to latitudinal redistribution of surface sources of NOx, CH_4 and CO, *Geophys. Res. Lett., 25*, 3931-3934, 1998.

Gupta, M.L., A.R. Douglass, S. Kawa and S. Pawson, Use of radon for evaluation of atmospheric transport models, Geophys. Res. Lett., submitted to Geophys. Res. Lett., 2003.

Hansen, J., M. Sato, R. Ruedy, A. Lacis and V. Oinas, Global warming in the twenth-first century: An alternative scenario, *Proc. Natl. Acad. Sci. USA, 97*, 9875-9880, 2000.

Holloway, T., A. M. Fiore and M. G. Hastings, Intercontinental Transport of Air Pollution: Will emerging science lead to a new hemispheric treaty?, *Environ. Sci. & Technol.* submitted, 2003.

Jacob, D.J. *et al.*, Evaluation and intercomparison of global atmospheric transport models using ^{222}Rn and other short-lived tracers, *J. Geophys. Res., 102*, 5953-5970, 1997.

Jaffe, D., H. Price, D. Parrish, A. Goldstein and J. Harris, Increasing background ozone during spring on the west coast of North America, *Geophys. Res. Lett., 30*(12), 1613, doi:10.1029/2003GL017024, 2003.

Pak, B.C. and M.J. Prather, CO_2 source inversions using satellite observations of the upper troposphere, *Geophys. Res. Lett., 28*, 4571-4574, 2001.

Prather, M. *et al.*, Fresh air in 21st century?, *Geophys.Res., Lett., 30*(2), 1100, doi:10.1029/2002GL016285, 2003.

Rodenbeck, C., S. Houweling, M. Gloor and M. Heimann, Time-dependent atmospheric CO_2 inversions based on interannually varying tracer transport, *Tellus, 55B*, 488-497, 2003.

Stohl, A., S. Eckhardt, C. Forster, P. James and N. Spichtinger, On the pathways and timescales of intercontinental air pollution transport, J. Geophys. Res., 107(D23), 4684, doi: 10.1029/2001JD001396, 2002.

Warwick, N.J., S. Bekki, K.S. Law, E.G. Nisbet and J.A. Pyle, The impact of meteorology on the interannual growth rate of atmospheric methane, *Geophys. Res., Lett., 29*(20), 1947, doi: 10.1029/2002GL015282, 2002.

Figure Captions

Figure 1 Global and regional surface emission distributions of radon-like tracers. Percent contributions from regional emissions to global source strength are also shown. See text for more details on the regional domain coverage.

Figure 2 Monthly and annual average tracer column burden discrepancy induced by meteorological variability between Y66 and Y67 over receptors R42 and R43.

Figure 3 Percent contributions of regional emissions to annual average vertical profiles of global tracer O for simulation Y66 over receptors R42 and R43.

Figure 4 Percent discrepancy between simulated annually averaged vertical profile of global tracer O for Y66 and Y67 over receptors R42 and R43.

Figure 5 Longitudinal variations in correlation coefficients for July monthly averaged absolute mixing ratios and associated spatial gradients from simulations Y66 and Y67.

Table 1: Annual mean and range of monthly averaged percent contribution of regional emissions to column burden over receptors R42 and R43 from simulation Y66

Source Region	R42		R43	
	Annual Mean	Monthly Range	Annual Mean	Monthly Range
Indo-China (A)	37.1	18.5-55.4	4.8	2.5-8.8
North America (B)	26.4	5.2-41.3	56.7	49.4-68.7
Europe (C)	4.1	1.7-8.0	1.8	0.73-4.9
Africa (D)	3.2	1.8-8.0	16.2	4.9-24.1
South America (E)	2.8	0.7-9.1	1.6	0.2-3.2
Russia (F)	10.9	6.6-16.6	1.2	0.8-2.4

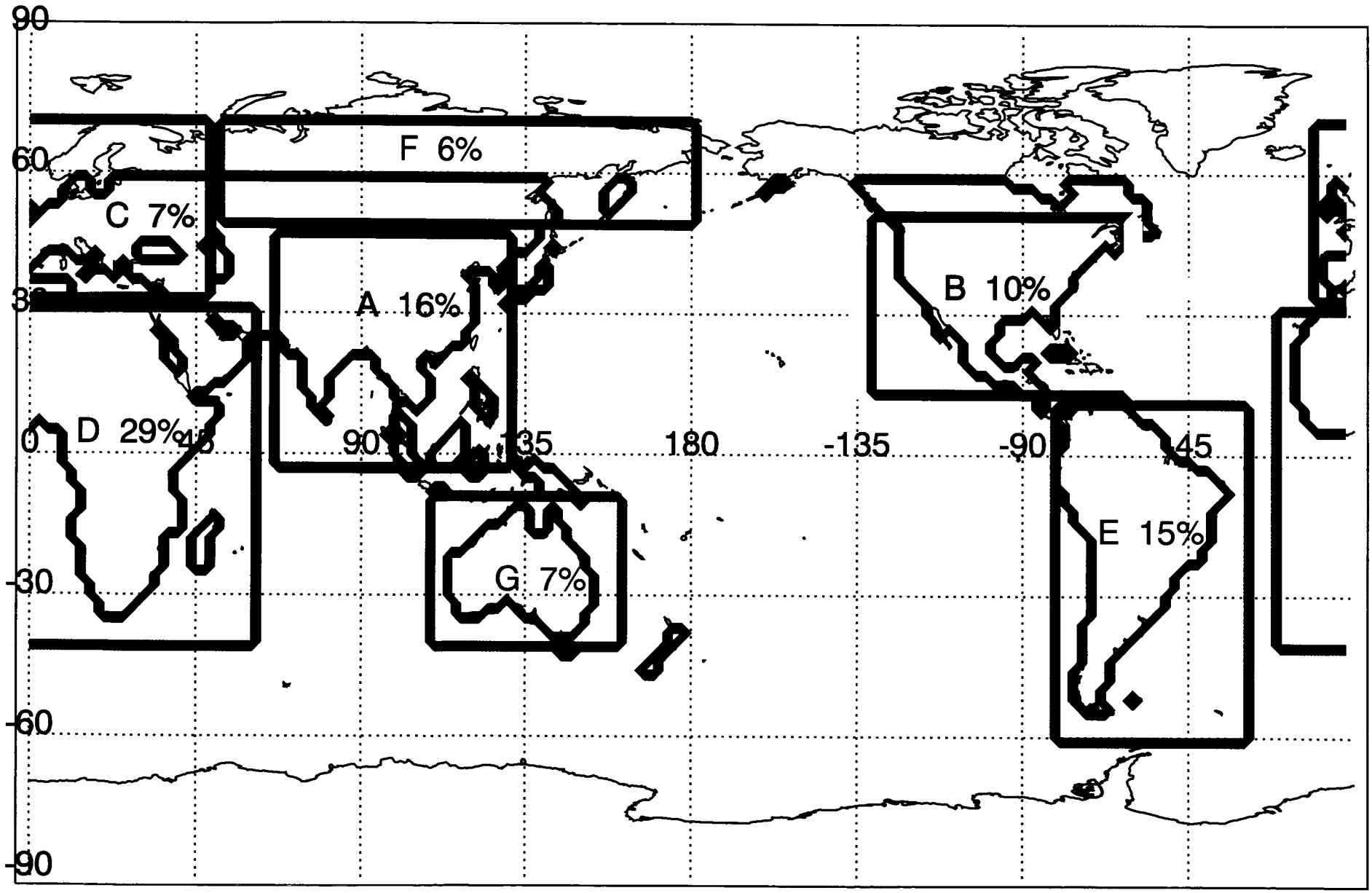

Fig 2

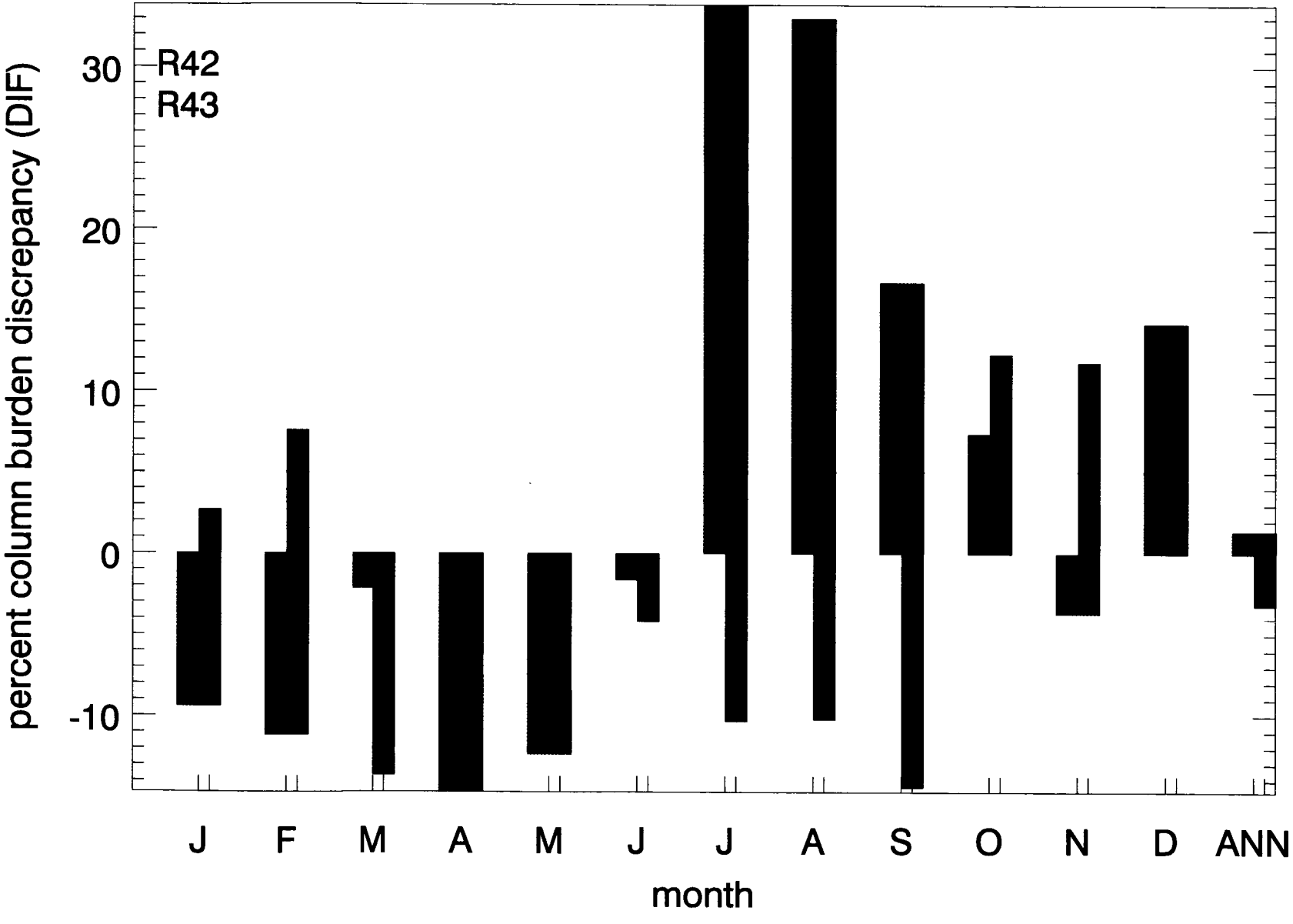
R42
R43
30
20
10
0
-10
percent column burden discrepancy (DIF)
J
F
M
A
M
J
J
A
S
O
N
D
ANN
month

Fig 2

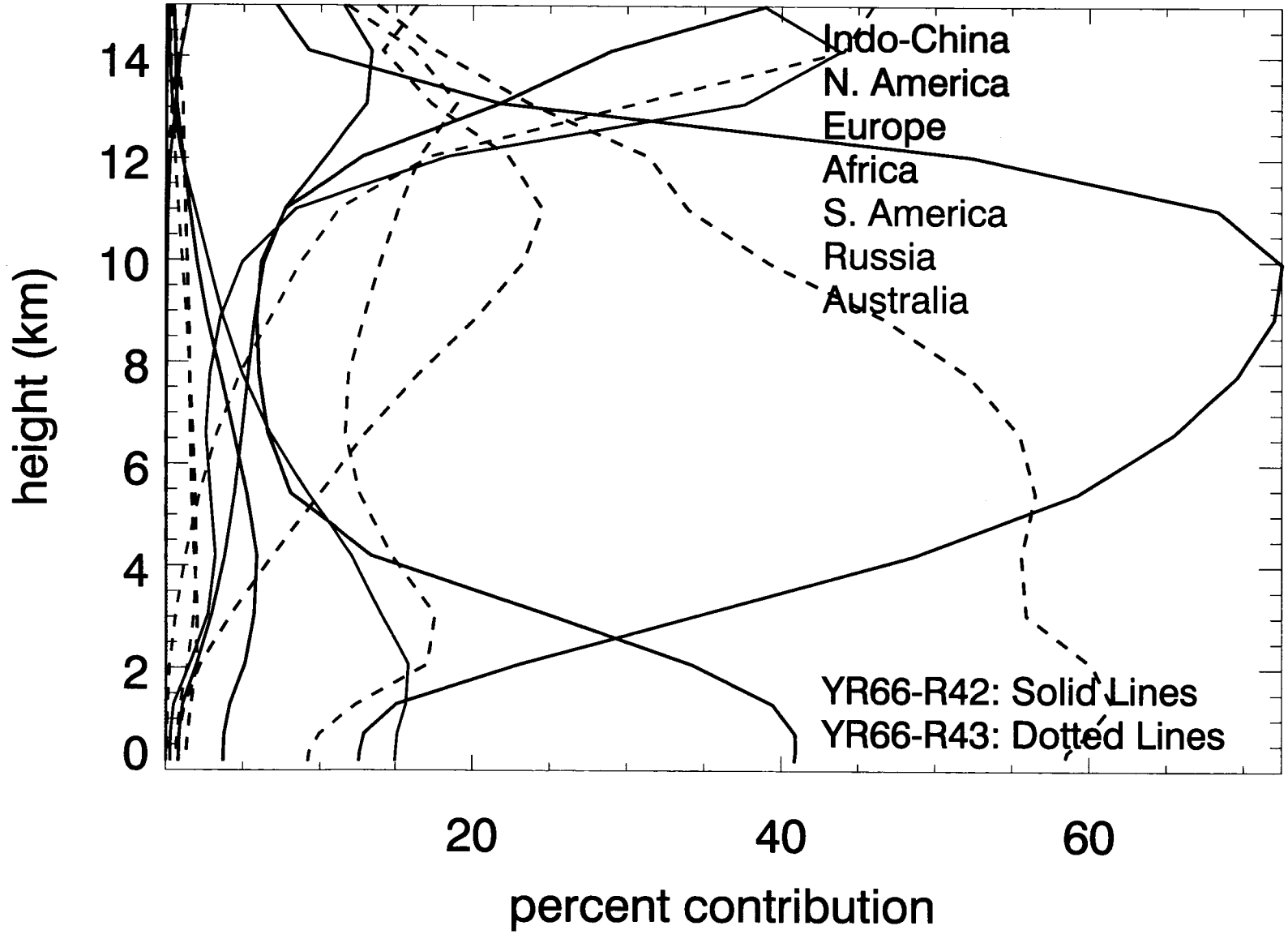
height (km)
0
2
4
6
8
10
12
14
20
40
60
percent contribution
Indo-China
N. America
Europe
Africa
S. America
Russia
Australia
YR66-R42: Solid Lines
YR66-R43: Dotted Lines

Fig 3

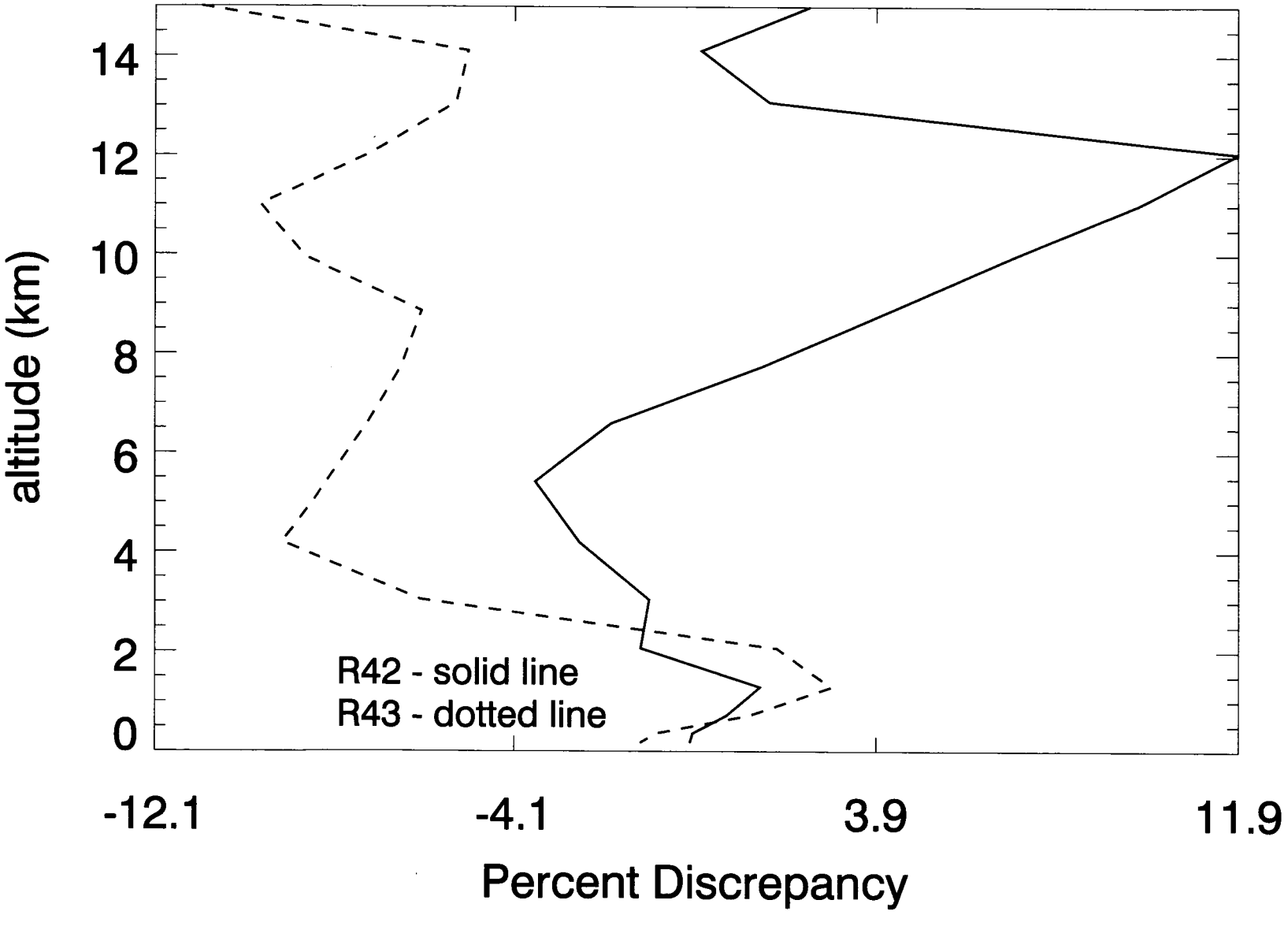
altitude (km)
14
12
10
8
6
4
2
0
R42 - solid line
R43 - dotted line
-12.1
-4.1
3.9
11.9
Percent Discrepancy

Fig 4

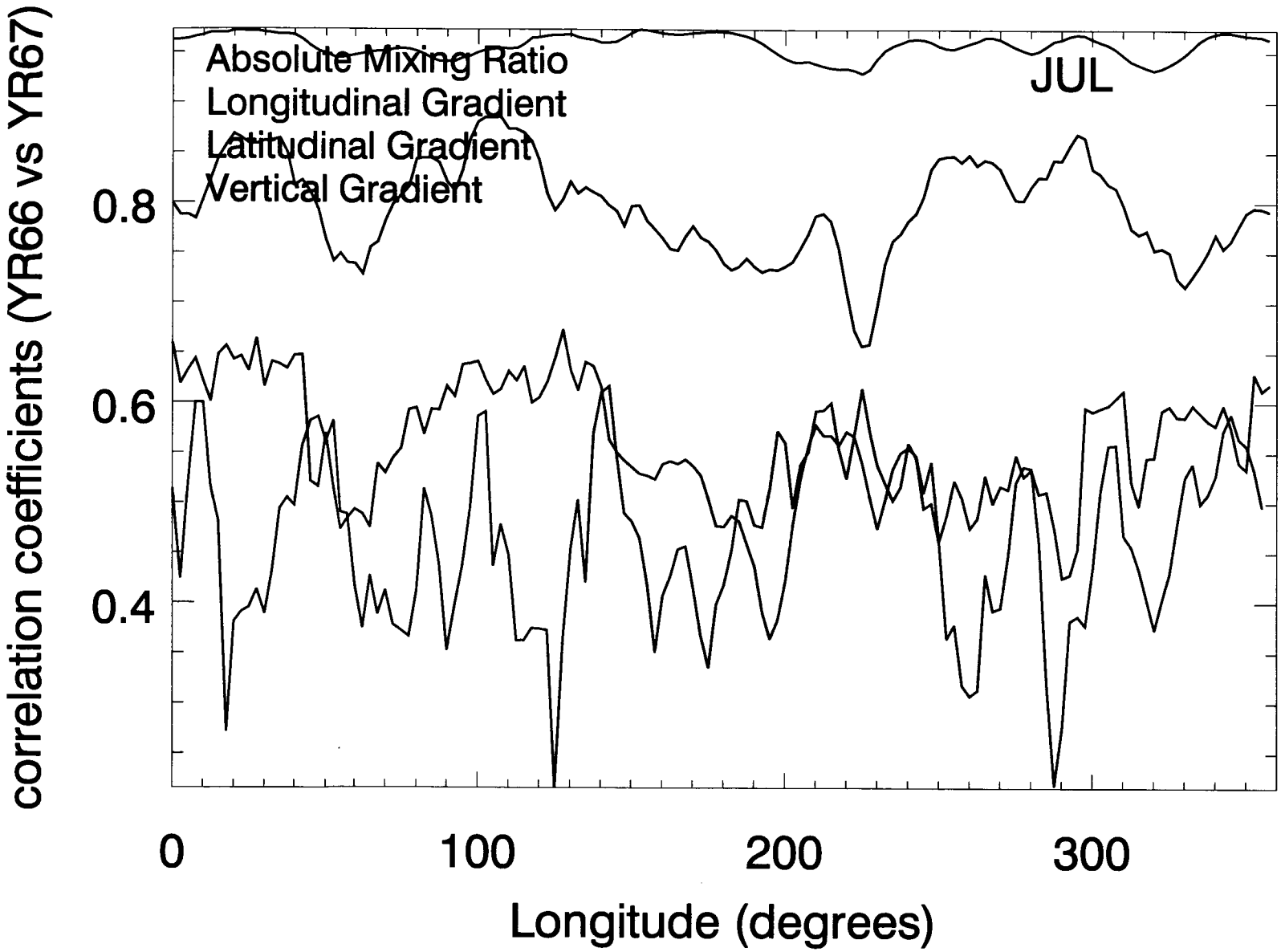
Absolute Mixing Ratio
Longitudinal Gradient
Latitudinal Gradient
Vertical Gradient
JUL
correlation coefficients (YR66 vs YR67)
0.8
0.6
0.4
0
100
200
300
Longitude (degrees)

fig 5